Plant Soil (2019) 436:123–140
https://doi.org/10.1007/s11104-018-03914-w

REGULAR ARTICLE

Soil substrates rather than gene abundance dominate DNRA capacity in the *Spartina alterniflora* ecotones of estuarine and intertidal wetlands

Xiaofei Li · Dengzhou Gao · Lijun Hou · Min Liu

Received: 18 September 2018 / Accepted: 11 December 2018 / Published online: 3 January 2019

Abstract

Background and aims Dissimilatory nitrate reduction to ammonium (DNRA) plays an important role in keeping nitrate retention as a more bioavailable form (ammonium) in estuarine and intertidal environments. However, the effects of soil abiotic and biotic characteristics on DNRA in *Spartina alterniflora* ecotones of estuarine and intertidal wetlands remain unclear.

Methods In this study, we used nitrogen isotope tracing and molecular approaches to investigate DNRA activity, and abiotic and biotic factors of both rhizosphere and non-rhizosphere soils in *Spartina alterniflora* ecotones of the Yangtze estuarine and intertidal wetlands.

Results DNRA varied significantly throughout the sampling sites, with potential rates of 0.53–3.57 nmol N g^{-1} h^{-1}. The rates of DNRA were significantly higher in rhizosphere than non-rhizosphere soils at the oligohaline sites. Salinity had more influence on DNRA activity than *Spartina alterniflora* at the brackish sites. Total organic carbon, nitrate, Fe (II) and sulfide were significantly correlated with DNRA rates and *nrfA* gene abundance. Soil substrates strongly affected DNRA activity in rhizosphere soil, while *nrfA* gene abundance was the predominant factor mediating DNRA activity in non-rhizosphere soil. DNRA contributed more to the total nitrate reduction at the brackish than oligohaline sites, suggesting that DNRA plays an important role in nitrate reduction in estuarine and intertidal wetlands.

Conclusions This study suggests that soil substrates rather than *nrfA* gene dominate DNRA activity in estuarine and intertidal wetlands after *Spartina alterniflora* invasion. Our results are helpful to understand the importance of soil characteristics changes induced by the exotic plant invasion to nitrogen cycling in estuarine and intertidal wetlands.

Keywords DNRA · *Spartina alterniflora* · Biotic variable · Environmental implications · Estuarine wetlands

Responsible Editor: Sven Marhan.

Electronic supplementary material The online version of this article (https://doi.org/10.1007/s11104-018-03914-w) contains supplementary material, which is available to authorized users.

X. Li
Key Laboratory for Humid Subtropical Eco-geographical Processes of the Ministry of Education, Fujian Normal University, Fuzhou 350007, China

X. Li
School of Geographical Sciences, Fujian Normal University, Fuzhou 350007, China

D. Gao · M. Liu (✉)
Key Laboratory of Geographic Information Science of the Ministry of Education, School of Geographic Sciences, East China Normal University, Shanghai 200241, China
e-mail: mliu@geo.ecnu.edu.cn

L. Hou (✉)
State Key Laboratory of Estuarine and Coastal Research, East China Normal University, Shanghai 200241, China
e-mail: ljhou@sklec.ecnu.edu.cn

Introduction

Estuarine and intertidal wetlands are important ecosystems for biogeochemical cycling, which have attracted an increasing attention at regional and global scales (Kirwan and Megonigal 2013; Greaver et al. 2016; Zhou et al. 2017; Van de Broek et al. 2018). Over the past few decades, global change and human activity are expected to cause sea level rise, seawater intrusion and exotic plant invasion in estuarine and intertidal wetlands (Church and White 2006; Rasmussen et al. 2013; Greaver et al. 2016), which in turn affect biogeochemical cycling in such susceptive ecosystems (Osborne et al. 2015; Zhou et al. 2017; Van de Broek et al. 2018). Elevated salinity as a result of seawater intrusion has been reported to stimulate microbial decomposition of organic carbon, leading to reduced carbon accumulation and increased carbon dioxide and methane emissions in estuarine and intertidal wetlands (Craft 2007; Morrissey et al. 2014; Liu et al. 2017a, b). Salinity increase induced by seawater intrusion may also enhance physiological stress on nitrogen cycling-associated microbial communities (Osborne et al. 2015), suggesting that the exposure to saline water may alter nitrogen cycling in estuaries. It has been reported that increasing salinity in coastal ecosystems enhances net nitrogen mineralization but decreases nitrification, denitrification and dissimilatory nitrate reduction to ammonium (DNRA) (Zhou et al. 2017). Many studies also indicate that high salinity increases nitrous oxide (N_2O) production through inhibition on denitrification reductase (Osborne et al. 2015; Zhou et al. 2017). In addition, a particular concern is the effect of vegetation invasion on estuarine and intertidal wetlands where it has been documented to alter the carbon biogeochemical cycling and increase organic matter storage (Liu et al. 2017a). A more recent study suggests that *Spartina alterniflora* invasion has a great influence on DNRA, denitrification and anammox activities (Gao et al. 2017). Overall, the changes of the biogeochemical cycling induced by seawater intrusion and vegetation invasion are usually considered the ecological and biological implications in the estuarine and intertidal wetlands. Therefore, the biogeochemical cycling and associated biogeochemical controls have become an increasing concern in estuarine and intertidal wetlands.

In recent decades, most of estuarine and intertidal wetlands have suffered from serious nitrogen pollution around the world, primarily because of the extensive agricultural and industrial activities (Deegan et al. 2012; Canion et al. 2014; Smith et al. 2015). Elevated nitrogen loading is a crucial driver leading to widespread occurrence of eutrophication, anoxia and water deterioration in estuarine and intertidal ecosystems (Canfield et al. 2010; Deegan et al. 2012). Nitrogen enrichment also affects nitrogen transformation processes in estuarine and intertidal wetlands (Roberts et al. 2014; Bernard et al. 2015; Hardison et al. 2015; Robertson et al. 2016; Gao et al. 2017). So far, many studies have concerned about denitrification and anammox, which are the dominant pathways of nitrogen loss from the estuarine and intertidal wetlands (Crowe et al. 2012; Fernandes et al. 2012; Hou et al. 2013; Hinshaw et al. 2017; Domangue and Mortazavi 2018). Recently, dissimilatory nitrate reduction to ammonium (DNRA) has been identified as an important nitrogen transformation pathway, which competes with denitrification and anammox for nitrate (Hardison et al. 2015; Robertson et al. 2016). Importantly, DNRA can retain nitrogen for recycling by converting nitrate into ammonium in estuarine and intertidal environments (Giblin et al. 2013; Roberts et al. 2014; Bernard et al. 2015). It has been documented that DNRA process is closely associated with salinity, temperature, organic matter, Fe (II), nitrate/nitrite, and sulfide in estuarine and intertidal environments (Gardner et al. 2006; Roberts et al. 2014; Bernard et al. 2015; Decleyre et al. 2015; Robertson et al. 2016). However, the role of plant communities in mediating DNRA is usually overlooked in the estuarine and intertidal wetlands. Thus, it still remains unclear about the importance of biotic variables induced by plant communities in regulating DNRA.

The vegetation in estuarine and intertidal wetlands plays an important role in enduring stormy waves, absorbing pollutants and facilitating sediment deposition (Hinshaw et al. 2017). Generally, *Phragmites australis*, *Cyperus malaccensis* and mangrove forest are the widespread plant communities in estuarine and intertidal wetlands (Zhang et al. 2010; Liu et al. 2017a). However, *Spartina alterniflora* is an exotic invasion vegetation in intertidal wetlands of China coastal zones, which has become an important plant community due to its great competition ability over indigenous plants and high growth capacity (Zuo et al. 2012; Liu et al. 2017a). Recently, vegetation has been reported to accelerate the accumulation of carbon and nitrogen, and to alter the extent and budget of nitrogen cycling (Henry et al. 2008; Zhang et al. 2010; He et al. 2016; Gao et al. 2017;

Hinshaw et al. 2017). The denitrification as a heterotrophic nitrogen transformation pathway can be enhanced by the organic matter at the high salinity condition (Canion et al. 2014; Osborne et al. 2015). In subtropical and tropical estuaries, DNRA can outcompete over denitrification in the organic matter-enriched and nitrate-limited environments, and thus becomes the dominant pathway of nitrate reduction (Gardner and McCarthy 2009; Roberts et al. 2014; Bernard et al. 2015; Zhou et al. 2017).

Microbial biomass and extracellular enzyme are crucial factors mediating microbial activity, which strongly affect the biogeochemical cycling (Morrissey et al. 2014; Jian et al. 2016; Xiao et al. 2018). Vegetation rhizosphere has a great influence on microbial enzyme activity through improving nutrient supply and ionic availability in soil environments (Dotaniya and Meena 2015). Microbial biomass and extracellular enzyme activity have been found to control the decomposition and storage of carbon and nitrogen (Morrissey et al. 2014; Jian et al. 2016). To date, there is limited information about the influence of microbial biomass and extracellular enzyme activity on nitrogen cycling, particularly DNRA, in estuarine and intertidal wetlands. DNRA is susceptible to C/N ratio (Hardison et al. 2015), and thus microbial biomass carbon and nitrogen are likely the important factors regulating the dynamics of DNRA. It is well known that intracellular DNA (iDNA) and extracellular DNA (eDNA) are dissimilar, of which eDNA comes from cell death and lysis or secretion of living cell (Nielsen et al. 2007; Pietramellara et al. 2009). It has also been suggested that nitrite reductase is a key marker mediating nitrate reduction processes (Dong et al. 2009). A pentaheme cytochrome C nitrite reductase (*nrfA*) is the major enzyme for performing fermentative DNRA, and thus the *nrfA* gene has been widely used to explore DNRA activity (Song et al. 2014; Decleyre et al. 2015; Smith et al. 2015). However, the iDNA and eDNA pools are usually influenced by the abiotic and biotic variables in aquatic environments, further leading to the changes in the ecological relevance on the biogeochemical cycling (Nielsen et al. 2007; Pietramellara et al. 2009). Therefore, it is worthy to elucidate the relative importance of *nrfA* gene in iDNA and eDNA in mediating the DNRA process.

In this study, nitrogen isotope tracing approach was used to investigate the dynamics of DNRA activity in *Spartina alterniflora* ecotones of estuarine and intertidal wetlands. The *nrfA* gene abundance, physicochemical properties, extracellular enzyme activity and microbial biomass were also measured to explore the relative influences of biotic and abiotic factors on DNRA activity. Furthermore, the ecological role of DNRA in nitrate reduction was also estimated under the condition of *Spartina alterniflora* invasion. This work provides novel insights into the biogeochemical controls on nitrogen cycling in *Spartina alterniflora* ecotones of estuarine and intertidal wetlands.

Materials and methods

Study area and sample collection

The Yangtze Estuary (121°5–122°30′E, 30°52–31°46'N) is situated in the center of China's coastal zone. Extensive intertidal wetlands along this estuary are well developed because large amounts of sediment are deposited during the interaction between the freshwater runoff and tidal current (Chen and Zhong 1998). *Spartina alterniflora* is the dominant invasion plant in intertidal wetlands of the Yangtze Estuary, with a growing season from March to October (Tang et al. 2011). In this study, six sites were selected in the intertidal wetlands of the Yangtze Estuary (Fig. 1), and the field survey was conducted in July 2016. At each site, the rhizosphere soil (RS) and non-rhizosphere soil (NRS) were collected from 3 replicate plots (30 cm × 30 cm) with *Spartina alterniflora*. Stem and leaf of *Spartina alterniflora* at each plot were harvested to estimate the aboveground biomass (AGB, fresh weight). Root of *Spartina alterniflora* determined by submerging each relevant soil was collected to estimate the belowground biomass (BGB, fresh weight). All samples were sealed in sterile plastic bags and transported to the laboratory on ice within 3 h. Upon return to the laboratory, each soil sample was homogenized thoroughly under helium and divided into two fractions. One fraction was immediately incubated to measure potential rates of DNRA and soil characteristics, and the other fraction was stored at −80 °C for subsequent molecular microbiology analysis.

Analyses of soil physicochemical properties, microbial biomass and extracellular enzymes

Soil pH and salinity were measured using Mettler-Toledo pH meter and YSI Model 30 conductivity meter,

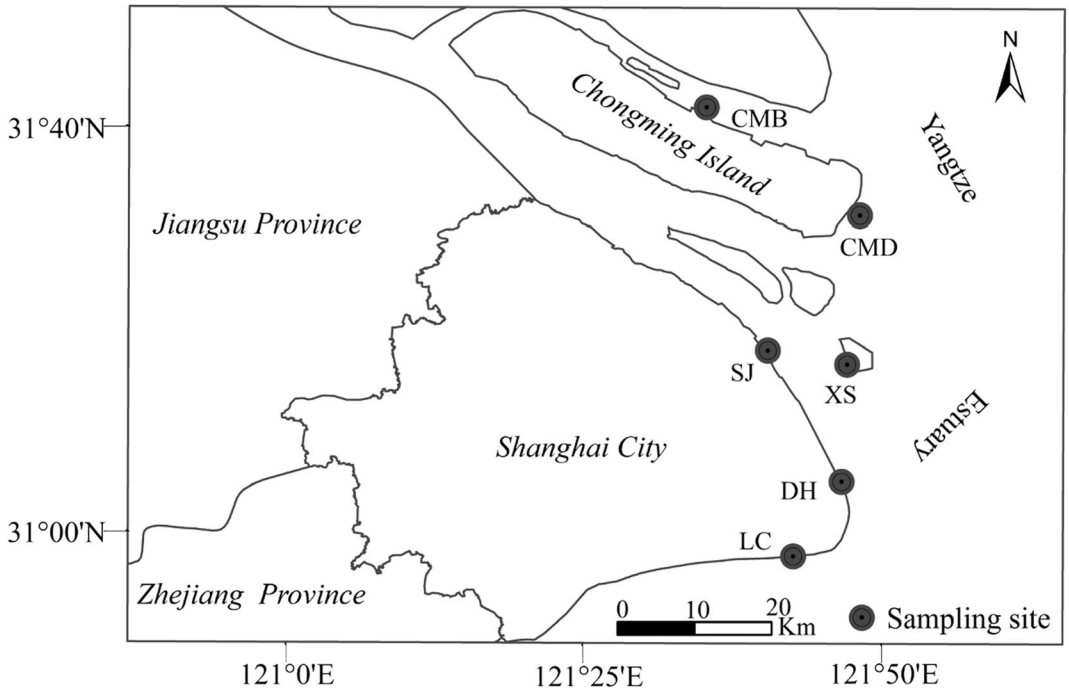

Fig. 1 Sampling sites in the intertidal wetlands of the Yangtze Estuary. CMB (Chongming Beitan), CMD (Chongming Dongtan), SJ (Sanjia), XS (Xiasha), DH (Donghai) and LC (Luchao)

respectively, after soil was mixed with CO_2-free deionized water at a ratio (*w*/*v*) of 1:2.5 (Hou et al. 2013). Soil particle-size was analyzed by laser granulometer (Beckman Coulter LS13320, USA). Total organic carbon (TOC) was determined using thermal combustion furnace analyzer (Elementar analyzer vario MaxCNOHS, Germany) after soil was leached by 1 mol L^{-1} HCl to remove carbonate (Hou et al. 2013). Soil NH_4^+, NO_3^- and NO_2^- were measured via continuous-flow nutrient autoanalyzer (SAN plus, Skalar Analytical B.V., Breda, Netherlands) after extraction with 2 mol L^{-1} KCl solution (Hou et al. 2013). Sulfide was determined by the method of Methylene Blue Spectrophotometry (Deng et al. 2015). The microbially oxidizable ferrous iron (Fe (II)) and microbially reducible ferric iron (Fe (III)) were determined according to the method described by Lovley and Phillips (1987). These physicochemical properties of each soil sample were measured in triplicate.

Soil microbial biomass carbon (MBC) and nitrogen (MBN) were determined using chloroform fumigation method (Vance et al. 1987; Brookes et al. 1985). In brief, 5 g soil was extracted with 20 mL of 0.5 mol L^{-1} K_2SO_4 solution, shaken for 30 min, and then centrifuged at 3000 rpm for 10 min. The supernatant was filtered through 0.45 μm pore-size filter. An additional 5 g soil was fumigated in dark at 28 °C with ethanol-free chloroform for 24 h, and then extracted with 0.5 mol L^{-1} K_2SO_4 solution. The dissolved organic carbon (DOC) and nitrogen (DON) in the extracted solution were determined using TOC-V_{CPH} analyzer (Shimadzu, Japan) and continuous flow auto-analyzer (SAN plus, Skalar Analytical B.V., Netherlands), respectively. Microbial biomass were obtained according to the differences in the DOC and DON before and after fumigation which were divided by 0.38 for MBC (Vance et al. 1987) and 0.45 for MBN (Brookes et al. 1985).

Soil extracellular enzymes including sucrase (SUC), cellulase (CEL), polyphenol oxidase (PPO), urease (URE), and catalase (CAT) were measured according to the methods slightly modified from Tabatabai (1994) and Du et al. (2014). These five enzymes were extracted with their substrates and reagents at optimal pH and incubated with gentle agitation at 37 °C for 24 h. Extracted solution was centrifuged, and the supernatant was transferred into a sterile tube. Subsequently, the supernatant was mixed with each developing agent for colorimetric analysis. The substrate and sample blanks receiving substrate and deionized water were performed in the colorimetric analysis. Absorbance in the

developing solution was detected using colorimetric plate reader (SpectraMax M5 Microplate Spectrophotometer; Molecular Devices Corporation, Sunnyvale, CA). Soil extracellular enzyme activities were calculated from the linear regressions between standard concentrations and absorbance according to the following equation:

$$E = A \times S \times V \times W^{-1} \times T^{-1} \quad (1)$$

where E (mg g^{-1} h^{-1}) is the extracellular enzyme activity, A is the absorbance, S (mg L^{-1}) is the slope of substrate concentration gradient versus absorbance, V (L) is the total volume of colorimetric solution, W (g) is the soil weight for extracellular enzyme extraction, and T (h) is the incubation time of extracellular enzyme extraction.

Measurement of DNRA rate

Potential rates of DNRA were measured by nitrogen isotope tracing method. Slurries of each sample were made with soil and helium-purged distilled water at a ratio (soil/water) of 1:7. The slurries were stirred homogeneously by magnetic stirrer for 25 min and transferred into helium-purged 12 mL vials (Labco Exetainers, UK). These vials were pre-incubated at room temperature for about 48 h to eliminate residual oxygen, nitrate, and nitrite, and then spiked with 0.1 mL $^{15}NO_3^-$ (final ^{15}N concentrations of about100 μmol L^{-1}). After spiked, these slurry vials were injected with 0.2 mL 50% $ZnCl_2$ to stop microbial activity at 0, 2, 4 and 8 h time-series incubation, respectively. Produced $^{15}NH_4^+$ from the DNRA process was oxidized into $^{29}N_2$ and $^{30}N_2$ with hypobromite iodine solution, and $^{29}N_2$ and $^{30}N_2$ were then quantified with membrane inlet mass spectrometry (MIMS, HPR-40, Hiden analytical, England) (Yin et al. 2014). In addition, $^{15}NH_4^+$ with known concentrations (0, 5, 10 and 20 μmol L^{-1}) was also oxidized with hypobromite iodine solution. A standard curve was thus constructed to calculate the concentrations of $^{15}NH_4^+$ produced from the incubation slurries. Potential rates of DNRA were calculated from concentration changes in the process-specific ^{15}N labeled product ($^{15}NH_4^+$) during the time-series incubation, according to the equation:

$$R_{DNRA} = S \times V \times W^{-1} \quad (2)$$

where R_{DNRA} (nmol ^{15}N g^{-1} h^{-1}) is the DNRA rate, S (nmol ^{15}N L^{-1} h^{-1}) is the slope of $^{15}NH_4^+$ concentrations versus incubation time, V (L) is the vial volume, and W (g) denotes the soil weight.

DNA extraction and PCR amplification

eDNA and iDNA in soils were extracted according to the method described by Mao et al. (2013). About 0.25 g soil was mixed with NaH_2PO_4 buffer (0.12 mol L^{-1}, pH 8.0) and polyvinyl polypyrrolidone (PVPP) to separate and dissolve the eDNA in soil. Extracted solution was shaken at 250 rpm for 10 min at 25 °C and then centrifuged at 10000 rpm for 10 min at 4 °C, and the supernatant was transferred into a sterile tube on ice. The soil pellet was extracted twice again according to the same approaches. The total supernatant of three extraction solution was filtered with 0.22 μm filter, and the filtrate was extracted using Power Soil DNA Isolation Kits (MOBIO, USA) to obtain the eDNA. Subsequently, the remaining soil pellet was extracted as the iDNA using Power Soil DNA Isolation Kits. Purity and concentrations of eDNA and iDNA were measured using a Nanodrop-2000 Spectrophotometer (Thermo, USA). Extracted DNA was then examined using 1.0% agarose gel electrophoresis.

The *nrfA* gene was amplified with primers *nrfA*-F1 (5'–GCN TGY TGG WSN TGY AA–3') and *nrfA*-7R1 (5'–TWN GGC ATR TGR CAR TC–3') (Mohan et al. 2004). PCR amplification was performed in 25 μL reaction mixture containing 1.0 μL of each primer (10 μM), 1 μL of template DNA, 12.5 μL of Taq PCR Master Mix (2×, with blue dye), and 9.5 μL of sterile distilled water. Thermal cycling was conducted under the conditions of an initial denaturing step at 94 °C for 5 min, and 94 °C for 30 s, 60 °C for 45 s and 72 °C for 1.5 min of 30 cycles, and then an extension step was carried out at 72 °C for 10 min (Smith et al. 2007). PCR products were identified by agarose gel electrophoresis (1.0% agarose) with ethidium bromide staining in 1× TAE buffer to ensure the correct size. Subsequently, target gene was purified with the DNA Purification Kit (Tiangen, China) and connected onto the pMD®19-T Vector that was conjugated into *Escherichia coli* DH5α.

Real-time quantitative polymerase chain reaction (qPCR)

Plasmids comprising *nrfA* gene fragment were extracted from *Escherichia coli* hosts with the SanPrep plasmid Mini Preparation Kit (Sangon, China) and used to

construct standard curves. The plasmid content was determined with the Nanodrop-2000 Spectrophotometer (Thermo, USA). The copy numbers of the *nrfA* gene in the extracted eDNA and iDNA were determined using the quantitative polymerase chain reaction (qPCR) approach. The *nrfA* gene fragment was amplified with the primers *nrfA*-2F ((5'–CAC GAC AGC AAG ACT GCC G–3') and *nrfA*-2R (5'–CCG GCA CTT TCG AGC CC–3') (Smith et al. 2007). The qPCR mixtures contained 12.5 μL of Maxima SYBR Green/RoxqPCR Master Mix (Fermentas, Lithuania), 1 μL of each primer (10 μmol L^{-1}, Sangon, China), 1 μL of template DNA, and 9.5 μL of sterile ddH_2O. The qPCR was performed under the reaction conditions of 2 min at 50 °C, 10 min at 95 °C, followed by 40 cycles of 30 s at 95 °C, 1 min at 60 °C, and 1 min at 72 °C. A standard curve was constructed from a series of 10-fold dilutions of a known copy number of plasmid DNA. The qPCR was conducted in triplicate by an ABI 7500 Sequence Detection System (Applied Biosystems, Canada) using the SYBR green qPCR method. A significantly linear relationship between the gene copy (log10) and threshold cycle (C_T) ($R^2 = 0.989$) and good amplification efficiency of 97.9% were observed to confirm the quality of qPCR. In all qPCR assays, three negative controls without DNA were conducted to exclude any possible contamination.

Statistical analyses

Statistical analyses in this study were performed using SPSS (version 19.0, SPSS), Canoco (version 4.5) and AMOS (version 24.0) software. A log10 transformation for *nrfA* gene abundance was utilized in all the statistical analyses. The mean comparison was conducted with one-way analysis of variance (ANOVA) using *LSD*'s test. Significant differences in soil characteristics between non-rhizosphere and rhizosphere soils were identified by *t*-test. Pearson's analyses were also used to evaluate the relationships among *nrfA* gene abundance, DNRA activity and soil variables. Principal component analyses (PCA) were used to identify the relationships among soil biotic and abiotic variables, DNRA rates, gene abundances, and extracellular enzyme activity. Redundancy analysis (RDA) was performed with Canoco software to clarify the influences of soil biotic and abiotic factors on DNRA rates and *nrfA* gene abundance. In addition, structural equation models (SEM) were constructed to reveal the indirect and direct effects of soil abiotic and biotic variables on DNRA rate and *nrfA* gene abundance.

Results

Soil characteristics

Soil characteristics are shown in Table 1. Soil salinity varied significantly across the sampling sites, with values of 0.7–6.5. Soil pH was slightly lower at the oligohaline than brackish sites. Soil TOC contents were significantly higher in rhizosphere than non-rhizosphere soils ($p < 0.05$), with values of 1.34–1.89% and 1.19–1.57%, respectively. Concentrations of NH_4^+ ranged from 0.37 to 1.22 μg g^{-1} in non-rhizosphere soils and from 0.42 to 1.77 μg g^{-1} in rhizosphere soils. NO_3^- contents were in the range of 0.75–2.51 μg g^{-1} and 0.94–2.30 μg g^{-1} in non-rhizosphere soils and rhizosphere soils, respectively. Contents of soil NO_2^- were significantly lower than NH_4^+ and NO_3^-, varying from 0.03 to 0.16 μg g^{-1}. Soil Fe (II) and Fe (III) contents ranged from 10.8 to 24.7 mg g^{-1} and 2.1 to 15 mg g^{-1}, respectively. Concentrations of sulfide were in the range of 0.65–2.31 μmol g^{-1} in non-rhizosphere soils and 0.62–4.12 μmol g^{-1} in rhizosphere soils. Soils were mainly composed of clay and silt, and the fine fractions with the grain size of <63 μm accounted for 80.5–99.8% of the total soils (Fig. S1). The above-ground biomass (AGB) and below-ground biomass (BGB) of *Spartina alterniflora* community ranged from 2.79 to 10.5 kg m^{-2} fresh weight and from 0.33 to 4.76 kg m^{-2} fresh weight, respectively.

Microbial biomass and extracellular enzyme activity

Microbial biomass carbon (MBC) ranged from 75.3 to 123.5 μg g^{-1} in non-rhizosphere soils and from 89.3 to 175.1 μg g^{-1} in rhizosphere soils (Table 2). Microbial biomass nitrogen (MBN) were higher in rhizosphere than non-rhizosphere soils, with values of 22.9–42.1 μg g^{-1} and 11.7–31.3 μg g^{-1}, respectively. Compared with non-rhizosphere soils, significantly higher contents of MBC and MBN in rhizosphere soils indicated that *Spartina alterniflora* rhizosphere could enhance the microbial biomass. The activities of all enzymes showed significant

Table 1 Soil physicochemical properties and biomass of *Spartina alterniflora* at the sampling sites

	CMD		CMB		XS		SJ		DH		LC	
	NRS	RS	NRS	RS	NRS	RS	NRS	RS	NRS	RS	NRS	RS
WC (%)	38.6	40.6	52.3	43.8	34.5	36.8	41.5	36.8	57.6	49.7	46.9	45.6
pH	8.0	7.7	7.7	7.4	7.7	7.2	8.3	8.6	8.1	7.9	8.2	8.0
Salinity	0.7	0.9	0.9	0.7	1.9	2.2	1.2	1.0	3.8	4.1	6.1	6.5
TOC (%)	1.23	1.55	1.19	1.34	1.31	1.58	1.57	1.89	1.31	1.45	1.32	1.38
NH_4^+ (μg g^{-1})	0.53	0.42	0.84	0.52	1.22	1.77	0.47	0.47	0.37	0.47	0.57	1.20
NO_3^- (μg g^{-1})	1.32	1.60	1.22	2.30	0.75	0.94	2.51	1.93	1.53	1.01	0.91	1.34
NO_2^- (μg g^{-1})	0.06	0.08	0.04	0.05	0.11	0.16	0.09	0.13	0.04	0.04	0.03	0.03
Fe (III) (mg g^{-1})	2.1	4.2	4.4	3.1	3.9	1.5	4.1	8.4	15.0	11.5	7.6	10.3
Fe (II) (mg g^{-1})	14.2	13.8	11.5	18.6	18.1	17.5	22.8	24.7	10.8	11.3	11.8	13.5
Sulfide (μmol g^{-1})	0.65	1.41	0.91	0.62	1.13	1.85	1.35	4.12	2.31	1.19	1.12	3.48
AGB (kg m^{-2})		9.74		7.2		2.79		10.5		5.76		3.23
BGB (kg m^{-2})		4.76		1.35		1.17		2.55		0.33		0.71

Values are the mean of triplicate soil samples

NRS non-rhizosphere soil, *RS* rhizosphere soil, *WC* water content, *TOC* total organic carbon, *MBC* microbial biomass carbon, *MBN* microbial biomass nitrogen, *AGB* above-ground biomass, *BGB* below-ground biomass

variations across the sampling sites (Table 2). The rates of measured enzymes were significantly higher in rhizosphere than non-rhizosphere soils. Rates of SUC ranged from 9.21 to 17.5 mg g^{-1} d^{-1} in non-rhizosphere soils and from 13.4 to 21.3 mg g^{-1} d^{-1} in rhizosphere soils. The maximal values of CEL and PPO activities were recorded at site SJ, and the minimal value at site CMD. CAT activity ranged from 1.73 to 3.55 mg g^{-1} d^{-1} in non-rhizosphere soils and from 2.28 to 4.16 mg g^{-1} d^{-1} in rhizosphere soils.

Potential rate of DNRA and associated *nrfA* gene abundance

Measured rates of DNRA ranged from 0.53 to 2.99 nmol g^{-1} h^{-1} in non-rhizosphere soils and from 1.07 to 3.57 nmol g^{-1} h^{-1} in rhizosphere soils (Fig. 2). At the oligohaline sites, DNRA rates were significantly higher in rhizosphere than non-rhizosphere soils ($p < 0.05$). In contrast, no significant difference was observed in DNRA rates between non-rhizosphere and rhizosphere soils at the brackish sites ($p > 0.05$).

Table 2 Microbial biomass carbon and nitrogen and extracellular enzyme activity in the soil samples

	CMD		CMB		XS		SJ		DH		LC	
	NRS	RS	NRS	RS	NRS	RS	NRS	RS	NRS	RS	NRS	RS
MBC (μg g^{-1})	76.5	98.2	102.7	138.6	94.2	136.4	123.5	175.1	81.9	92.5	75.3	89.3
MBN (μg g^{-1})	11.7	23.4	16.2	30.8	28.4	33.6	31.3	42.1	13.5	27.4	15.8	22.9
SUC (mg g^{-1} d^{-1})	13.0	14.9	9.21	13.4	10.5	18.6	17.5	21.3	14.5	14.2	13.9	13.8
CEL (mg g^{-1} d^{-1})	0.24	0.31	0.18	0.24	0.24	0.42	0.35	0.47	0.21	0.34	0.26	0.33
PPO (mg g^{-1} d^{-1})	0.36	0.54	0.44	0.44	0.45	0.67	0.49	0.72	0.41	0.51	0.39	0.44
URE (mg g^{-1} d^{-1})	2.42	2.26	2.54	1.34	2.27	3.45	1.15	1.11	1.01	1.16	1.15	2.14
CAT (mg g^{-1} d^{-1})	3.19	3.54	2.68	2.28	3.22	4.16	3.55	3.14	1.86	3.30	1.73	2.77

Values are the mean of triplicate soil samples

MBC microbial biomass carbon, *MBN* microbial biomass nitrogen, *SUC* sucrose, *CEL* cellulose, *PPO* polyphenol oxidase, *URE* urease, *CAT* catalase

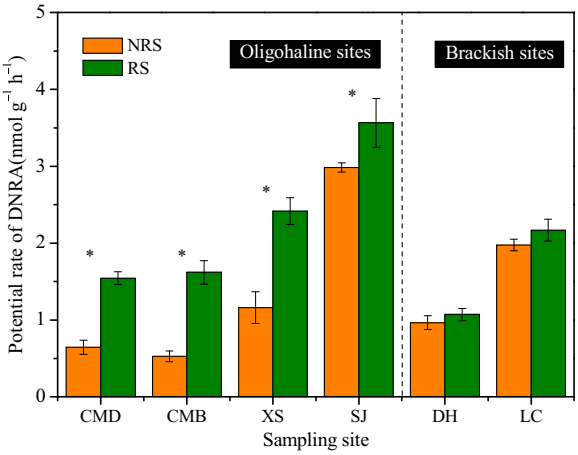

Fig. 2 Potential rates of DNRA in the soil samples of estuarine and intertidal wetlands. Bars in column indicate the standard deviation of the triplicate values. Asterisks show the significant difference in DNRA rates between non-rhizosphere soils (NRS) and rhizosphere soils (RS) ($p < 0.05$, *t*-test)

Abundance of *nrfA* gene in iDNA increased from 3.96×10^7 to 8.65×10^7 copies g^{-1} in non-rhizosphere soils and from 4.80×10^7 to 9.26×10^7 copies g^{-1} in rhizosphere soils (Fig. 3). The maximal *nrfA* gene abundance in iDNA was observed at site SJ, while the minimal value was recorded at sites CMD and XS. Abundance of *nrfA* gene in eDNA ranged from 2.35×10^6 to 3.95×10^6 copies g^{-1} in non-rhizosphere soils and from 1.96×10^6 to 3.42×10^6 copies g^{-1} in rhizosphere soils (Fig. 3). There was no significant difference in *nrfA* gene abundance in eDNA between rhizosphere and non-rhizosphere soils across the sampling sites. In this study, the *nrfA* gene abundance in iDNA was significantly correlated with the DNRA rates in both non-rhizosphere ($R^2 = 0.77$, $p < 0.01$) and rhizosphere soils ($R^2 = 0.59$, $p < 0.01$) (Fig. 4). However, no significant correlation was observed between DNRA rates and *nrfA* gene abundance in eDNA ($p > 0.05$).

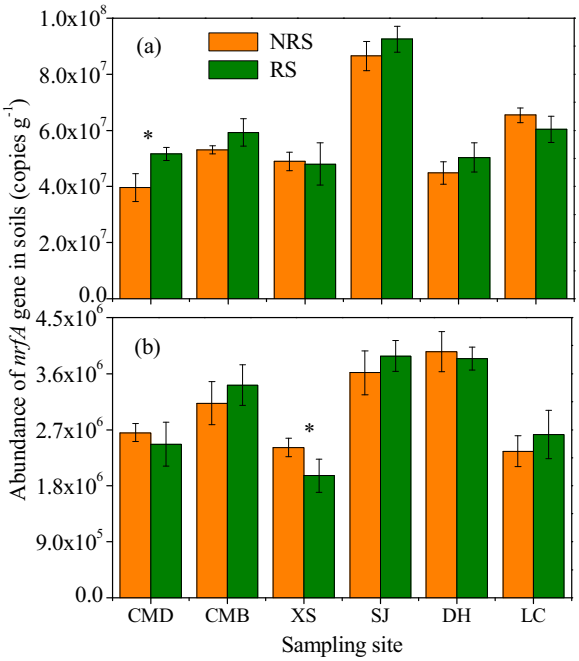

Fig. 3 Abundances of *nrfA* gene in iDNA (**a**) and eDNA (**b**) from the rhizosphere soils (RS) and non-rhizosphere soils (NRS). Bars in column indicate the standard deviation of the triplicate values. Asterisk show the significant difference in *nrfA* gene abundance between NRS and RS ($p < 0.05$, *t*-test)

Effects of abiotic and biotic variables on DNRA rate and *nrfA* gene abundance

Table 3 shows the relationships of soil abiotic properties with DNRA rates and *nrfA* gene abundance. The DNRA rates were related to pH, TOC, NH_4^+ and Fe (II) in non-rhizosphere soils ($p < 0.05$), while they had close correlations with pH, TOC, NO_2^-, Fe (II) and sulfide in rhizosphere soils ($p < 0.05$). Of these measured parameters, TOC and Fe (II) showed positive correlations with *nrfA* gene abundance in iDNA from non-rhizosphere soils ($p < 0.05$). However, pH, TOC, NH_4^+, Fe (II), and sulfide were the predominant properties affecting the *nrfA* gene abundance in iDNA from rhizosphere soils. The abundance of *nrfA* gene in eDNA was significantly correlated with NO_3^- ($r = 0.87$, $p < 0.01$) and

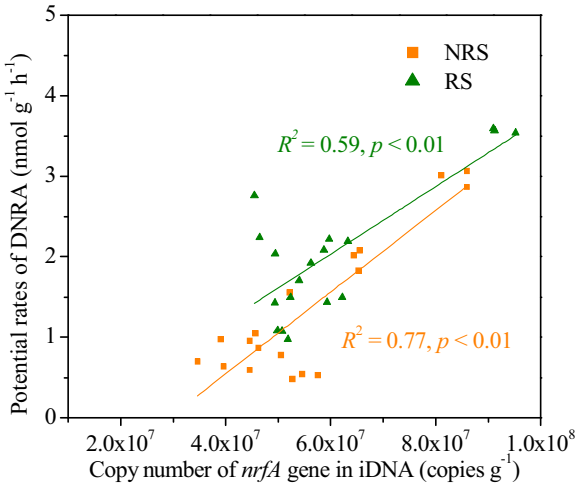

Fig. 4 Relationships of *nrfA* gene abundances in iDNA with potential DNRA rates in rhizosphere soils (RS) and non- rhizosphere soils (NRS)

Table 3 Pearson's correlations of soil abiotic properties with DNRA rates and *nrfA* gene abundance

		Salinity	pH	TOC	NH_4^+	NO_3^-	NO_2^-	Fe (III)	Fe (II)	Sulfide
Non-rhizosphere soil										
DNRA rate	*r*	0.38	0.71	0.83	−0.53	−0.31	0.28	−0.04	0.68	0.17
	p	0.12	0.001	0.00	0.02	0.21	0.25	0.88	0.002	0.51
nrfA in iDNA	*r*	0.27	0.45	0.67	−0.52	−0.43	0.14	−0.14	0.52	0.01
	p	0.29	0.06	0.003	0.03	0.08	0.59	0.59	0.03	0.98
nrfA in eDNA	*r*	−0.36	−0.39	0.21	0.25	0.87	0.76	0.04	0.47	0.32
	p	0.14	0.11	0.39	0.31	0.00	0.00	0.89	0.051	0.20
Rhizosphere soil										
DNRA rate	*r*	0.01	0.59	0.73	0.005	−0.10	0.54	−0.07	0.81	0.82
	p	0.96	0.01	0.001	0.98	0.70	0.02	0.77	0.00	0.00
nrfA in iDNA	*r*	0.13	0.83	0.59	−0.56	−0.25	0.03	0.29	0.77	0.72
	p	0.61	0.00	0.01	0.02	0.32	0.89	0.25	0.00	0.001
nrfA in eDNA	*r*	−0.36	−0.22	0.29	−0.01	0.17	0.68	−0.10	0.37	−0.12
	p	0.14	0.38	0.24	0.97	0.50	0.002	0.71	0.13	0.63

NO_2^- ($r = 0.76$, $p < 0.01$) in non-rhizosphere soils, but it was only related to NO_2^- ($r = 0.68$, $p < 0.01$) in rhizosphere soils. Microbial biomass and extracellular enzyme activity had strong influences on DNRA rates and associated *nrfA* gene abundance (Table 4). Significant correlations of DNRA rates with MBC, MBN, SUC, CEL and PPO were observed in both non-rhizosphere and rhizosphere soils (all $r > 0.48$, $p < 0.05$). The *nrfA* gene abundance in iDNA was positively related to MBC, MBN, URE, CEL and PPO in non-rhizosphere soils (all $r > 0.48$, $p < 0.05$) and to MBC, SUC, URE and PPO in rhizosphere soils (all $|r| > 0.53$, $p < 0.05$). In addition, the RDA analysis revealed that TOC, Fe (II), sulfide and NO_3^- had the close correlations with DNRA rates (Fig. S2).

Based on Pearson's correlation analyses, DNRA rates showed significantly positive relationships with TOC, NO_3^-, Fe (II), sulfide, *nrfA* gene, MBC, MBN, SUC, CEL and PPO (Tables 3 and 4). In addition, soil salinity varied significantly across the sampling sites, thus salinity was also identified in the SEM. Therefore, the SEM was constructed to explore the direct and indirect effects of these abiotic and biotic parameters on DNRA rates. In these models, 81% and 72% of DNRA rates in non-rhizosphere and rhizosphere soils could be explained by these variables, respectively (Fig. 5). For non-rhizosphere soils, salinity and MBC had strong influences on *nrfA* gene abundance. In addition, salinity, *nrfA* gene, Fe (II) and SUC showed significant influences on DNRA rates (Fig. 5a). In addition, DNRA rates were also indirectly impacted by salinity, TOC, MBC and MBN in non-rhizosphere soils (Table S1). For rhizosphere soils, salinity and MBC had significant influences on *nrfA* gene abundance (Fig. 5b). The *nrfA* gene abundance, salinity and PPO had strongly negative impacts on DNRA rates, but sulfide and CEL positively influenced DNRA rates in rhizosphere soils. In addition, DNRA rates were not only directly affected by TOC, NO_3^-, and Fe (II), but also were indirectly affected by salinity, TOC, MBC and MBN (Table S1).

Principal component analysis

In the present study, three principal components were identified by the principal component analyses of soil DNRA rates, abiotic and biotic variables (Table 5). The *nrfA* gene abundance and extracellular enzyme activity explained 72.0% of the total variations. The abiotic variables (TOC, NO_3^-, NO_2^-, Fe (II) and sulfide), biotic variables (MBC, MBN, SUC, CEL PPO and CAT), DNRA rates and *nrfA* gene abundance in iDNA were strongly correlated with PC 1, which explained 43.1% of the variations (Table 5 and Fig. 6b). In addition, the

Table 4 Pearson's correlations of DNRA rates and *nrfA* gene abundance with soil microbial biomass and enzyme activities

		MBC	MBN	SUC	CEL	PPO	URE	CAT
Non-rhizosphere soil								
DNRA rate	*r*	0.49	0.65	0.78	0.86	0.49	−0.68	0.19
	p	0.04	0.003	0.00	0.00	0.04	0.002	0.46
nrfA in iDNA	*r*	0.62	0.63	0.46	0.60	0.47	0.49	0.12
	p	0.006	0.005	0.06	0.00	0.05	0.04	0.64
nrfA in eDNA	*r*	0.39	0.61	−0.12	0.08	0.51	0.09	0.42
	p	0.11	0.07	0.65	0.76	0.03	0.71	0.08
Rhizosphere soil								
DNRA rate	*r*	0.71	0.44	0.80	0.72	0.66	0.02	0.10
	p	0.001	0.07	0.00	0.001	0.003	0.94	0.70
nrfA in iDNA	*r*	0.59	0.36	0.54	0.41	0.36	−0.58	−0.39
	p	0.01	0.14	0.02	0.09	0.14	0.01	0.11
nrfA in eDNA	*r*	0.57	0.73	0.2	0.44	0.58	0.21	0.42
	p	0.01	0.001	0.03	007	0.01	0.41	0.08

scatter plot of PC 1 indicated strong difference in the soil variables between non-rhizosphere and rhizosphere soils, with non-rhizosphere soils clustering on the left side of the y-axis and rhizosphere soils clustering on the right side of the y-axis (Fig. 6a). This difference suggested the effects of vegetation rhizosphere on soil variables. Soil pH, salinity, NH_4^+, Fe (III), URE and CAT were significantly correlated with PC 2 (Table 5 and Fig. 6b), which explained 19.3% of the variations. PC 2 also showed the spatial distribution of the sampling sites, with higher DNRA rates and associated abiotic and biotic parameters close to the x-axis (Fig. 6a). Soil salinity, NH_4^+, URE and *nrfA* gene abundance in eDNA were also closely correlated with PC 3, which explained only 9.6% of the variations.

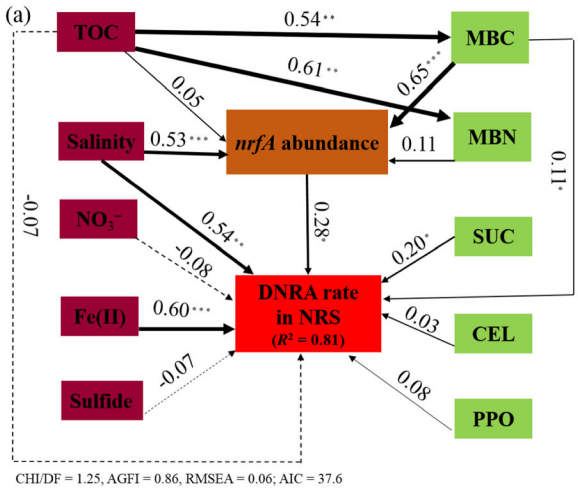

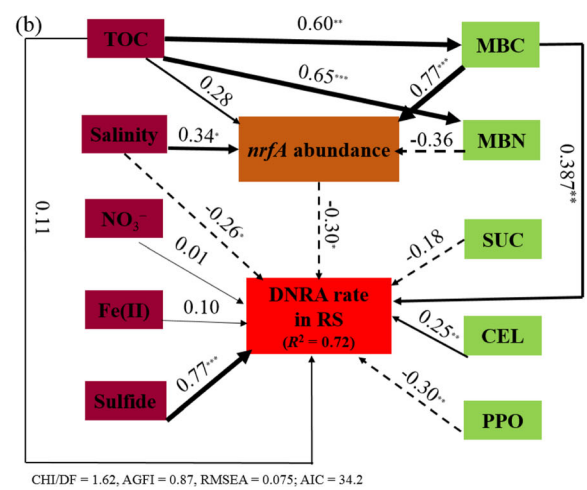

Fig. 5 Path diagrams demonstrating the direct and indirect effects of abiotic and biotic factors on DNRA rates and *nrfA* gene abundance in iDNA from non-rhizosphere soils (NRS) (**a**), DNRA rates and *nrfA* gene abundance in iDNA from rhizosphere soils (RS) (**b**). The parameters in brownish red and green boxes are abiotic and biotic variables, respectively. The width of the arrows is proportionate to the strength of the path coefficients adjacent with numbers. Solid and dashed lines represent positive and negative paths, respectively. The R^2 denotes the proportion of variance that could be explained by the corresponding variable in the model. Significance levels are as follows: $*p < 0.05$, $**p < 0.01$ and $***p < 0.001$

Table 5 Loading matrix of correlation coefficients for soil abiotic and biotic variables, DNRA rates, and *nrfA* gene abundances with principal components (PC 1, PC 2 and PC 3)

	PC 1	PC 2	PC 3
Abiotic variables			
pH	0.24	0.81*	0.02
Salinity	−0.10	0.72*	0.52*
TOC	0.91*	0.21	0.13
NH_4^+	0.24	−0.67*	0.64*
NO_3^-	0.78*	−0.04	−0.36
NO_2^-	0.80*	−0.49	−0.05
Fe (III)	−0.21	0.73*	−0.15
Fe (II)	0.84*	0.04	−0.11
Sulfide	0.58*	0.49	0.21
Biotic variables			
MBC	0.86*	−0.02	−0.33
MBN	0.87*	−0.09	−0.35
SUC	0.84*	0.25	0.05
CEL	0.87*	0.15	0.27
PPO	0.90*	−0.06	0.06
URE	0.20	−0.76*	0.55*
CAT	0.56*	−0.60*	0.11
nrfA in iDNA	0.63*	0.38	0.28
nrfA in eDNA	0.32	−0.38	−0.58*
DNRA process			
DNRA rate	0.87*	0.33	0.14

Significant values are indicated with asterisk (*)

Discussion

Distribution and biogeochemical controls of DNRA in estuarine and intertidal wetlands

Nitrogen cycling has attracted an increasing attention because nitrogen pollution has led to serious environmental problems in aquatic environments. DNRA is an important nitrogen transformation pathway by which nitrate is reduced to ammonium. This process occurs in most of estuarine and coastal environments and contributes to the nitrogen retention (An and Gardner 2002; Gardner et al. 2006; Gardner and McCarthy 2009; Dong et al. 2011; Dunn et al. 2013), thus further aggravating eutrophication in these aquatic ecosystems (Roberts et al. 2014; Bernard et al. 2015; Robertson et al. 2016). However, estuarine and intertidal wetlands provide favorable conditions for DNRA occurrence, because of vegetation invasion and increased nitrogen loading (Koop-Jakobsen and Giblin 2010; Hardison et al. 2015; Gao et al. 2017). Therefore, DNRA plays an increasing role in mediating nitrate reduction under changing environmental conditions in estuarine and intertidal wetlands.

Although many studies have documented the DNRA process (Dong et al. 2011; Roberts et al. 2014; Bernard et al. 2015; Robertson et al. 2016; Hinshaw et al. 2017), there is limited information about the importance of biotic parameters in controlling DNRA in estuarine and intertidal wetlands. In the present study, our nitrogen isotope tracing experiments examined DNRA activity in rhizosphere and non-rhizosphere soils from the *Spartina alterniflora* ecotones of estuarine and intertidal wetlands. In addition, the *nrfA* gene abundance and extracellular enzyme activity also provided both genetic information and microbial activity capacity for better explanation about the effects of biotic variables on DNRA activity. The spatial variations in DNRA rates in rhizosphere and non-rhizosphere soils suggested that *Spartina alterniflora* invasion enhances DNRA activity and plays a crucial role in regulating DNRA at the oligohaline sites. On the contrary, salinity likely inhibits DNRA activity, and thus *Spartina alterniflora* invasion may have a weak influence on DNRA at the brackish sites. Generally, DNRA rates were higher in rhizosphere than non-rhizosphere soils, mainly because rhizosphere soil has a stable microenvironment and provides abundant substrates and favorable conditions for DNRA microorganisms (Hinshaw et al. 2017; Gao et al. 2017).

In dynamic estuarine and intertidal environments, the interaction between freshwater and seawater can cause substantial alterations of nutrients, redox status, environmental properties, further resulting in a great fluctuation of nitrate reduction capability (Dong et al. 2011). The rates of DNRA measured in this study were comparable to the data available from other estuarine and coastal environments, but the percentage of DNRA in total nitrate reduction varied with a wide range across these ecosystems (Table S2) (Christensen et al. 2000; An and Gardner 2002; Gardner et al. 2006; Dong et al. 2009, 2011; Roberts et al. 2014; Yin et al. 2014; Robertson et al. 2016; Gao et al. 2017). This comparison reflected that DNRA competes with denitrification and anammox for nitrate and thus the importance of DNRA varies greatly across different estuarine and intertidal environments (Koop-Jakobsen and Giblin 2010; Hardison et al. 2015). Many studies have identified that the increasing salinity from freshwater to brackish

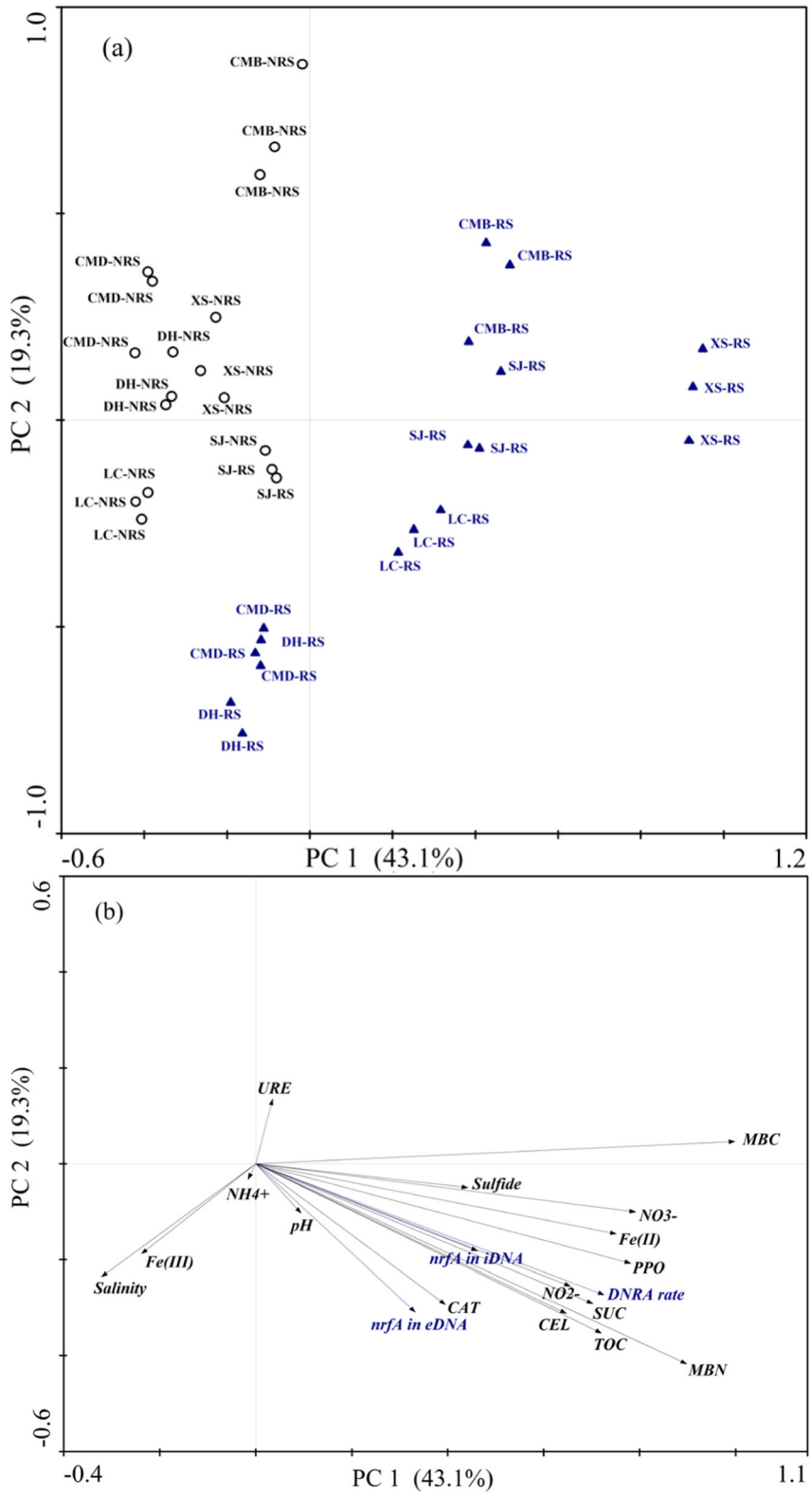

Fig. 6 Principal components (PC 1 and PC 2) depicting spatial and rhizospheric effects for abiotic and biotic variables, DNRA rates and abundances of *nrfA* gene in eDNA and iDNA shown by a scatter plot of component scores for rhizosphere soils (RS, open circle) and non-rhizosphere soils (NRS, solid triangle) (**a**) and PCA variables (**b**)

conditions along the estuarine gradient can favor DNRA over denitrification because nitrate availability decreases with the salinity (Giblin et al. 2010; Zhou et al. 2017). In addition, the increase of salinity can enhance the sulfate reduction into sulfide, which in turn stimulates sulfide-fueled DNRA (Giblin et al. 2010, 2013). However, the decrease in DNRA rates was observed at the brackish sites DH and LC. This was likely attributed to the negative effects of salinity on organic carbon, NO_3^- and Fe (II) availability, which in turn suppressed the activity of DNRA bacteria (Noe et al. 2013; Zhou et al. 2017). Therefore, the mechanism underlying the interaction between DNRA and salinity in estuarine and intertidal wetlands is likely complex, because the change in salinity is often coupled with other factors which also affect DNRA.

The environmental parameters in estuarine and intertidal wetlands are highly complex and variable, and thus the primary factors regulating the DNRA process vary in space and time (Smith et al. 2007; Gardner et al. 2006; Dong et al. 2011; Dunn et al. 2013; Bernard et al. 2015; Robertson et al. 2016; Zhou et al. 2017). In this study, compared to non-rhizosphere soils, higher DNRA capacity in rhizosphere soils may be attributed to the increased TOC, nitrate, Fe (II) and sulfide availability induced by *Spartina alterniflora* invasion (Table 3). It has been reported that fermentation is the main pathway of DNRA, which can be favored in high organic matter condition (Hardison et al. 2015). Besides, organic matter can also stimulate microbial activity and provide medium for DNRA microorganisms. Therefore, organic matter is a crucial factor regulating DNRA in estuarine and intertidal wetlands, which is supported by the significant correlations of TOC with DNRA rates and *nrfA* gene abundance in this study. Previous studies have revealed that the DNRA process strongly depends on nitrate content (An and Gardner 2002; Gardner et al. 2006; Dong et al. 2009, 2011; Bernard et al. 2015; Hardison et al. 2015). DNRA can compete for nitrate with other nitrate reduction processes especially denitrification, and thus DNRA can outcompete denitrification if high contents of organic carbon and nitrate-limited are present in the environments. The RDA analysis also supported the strong effect of nitrate on DNRA rates (Fig. S2). The ratio of organic carbon to nitrate can affect the DNRA and denitrification, and DNRA is generally favored over denitrification under the high organic carbon and low nitrate conditions (Hardison et al. 2015). In addition, it has been reported that increasing salinity tends to favor DNRA over denitrification (Giblin et al. 2010), because the enhanced reduction of sulfate to sulfide in response to increasing salinity can fuel DNRA. Therefore, the microbial organisms carrying out sulfide-induced DNRA may gain advantage over heterotrophic denitrifiers when exposed to high sulfide concentrations in estuarine and intertidal wetlands. The DNRA dynamics may also be linked to the difference in Fe (II) availability, which supports the Fe (II)-fueled nitrate reduction into ammonium (Giblin et al. 2010; Roberts et al. 2014; Robertson et al. 2016). In our study, higher DNRA rates were observed at the sites enriched with Fe (II) and sulfide, even though TOC contents were lower. However, soil abiotic properties were coupled with each other (Table S3), making them more difficult to explain the biogeochemical controls on DNRA.

Considering the microbial influence on DNRA, we observed that *nrfA* gene abundance in iDNA played a significant role in mediating DNRA (Fig. 4), suggesting that the microbial community is an important factor for DNRA activity (Giblin et al. 2013; Decleyre et al. 2015). Additionally, TOC and MBC were significantly correlated with *nrfA* gene abundance in iDNA (Table 3), which partly provided the evidence for the occurrence of fermentative DNRA in estuarine and intertidal wetlands. There were more abiotic variables affecting *nrfA* gene abundance in iDNA from rhizosphere soils compared to non-rhizosphere soils (Table 3), further supporting that DNRA activity would be favored in rhizosphere soils. In addition, the relationship between *nrfA* gene abundance in iDNA and DNRA rates was weaker in rhizosphere than in non-rhizosphere soils (Fig. 4), which in turn evidenced the more importance of soil substrates to DNRA activity than *nrfA* gene abundance in rhizosphere soil. Some abiotic variables, especially TOC, were significantly related to microbial biomass and extracellular enzyme activity (Table S4), indicating that microbial activity had also influences on DNRA rates and *nrfA* gene abundance in iDNA (Table 4 and Table S5). Relatively higher bacterial abundance was observed at the sites where DNRA rates were generally greater (Fig. S3 and Fig. 2), suggesting that microbial metabolism potential would also affect DNRA. Therefore, we argue that plant-controlled substrate availabilities were a crucial mechanism driving the differences in DNRA activity and *nrfA* gene abundance between rhizosphere and non-rhizosphere soils. The soil clay was significantly correlated with *nrfA* gene abundance in

eDNA (Table S6), because TOC is usually enriched in clay. The close relationships of eDNA with clay and TOC were observed (Table S7 and Fig. S4), showing the adsorption of eDNA by clay and organic matter (Nielsen et al. 2007). In addition, pH, ionic strength and solutes are also the main factors regulating the fate of eDNA in aquatic environments (Saeki et al. 2010). Dell'Anno et al. (2002) reported that eDNA may play an important role in the biogeochemical cycling, because it affects gene transfer via natural medium transportation and provides nitrogen and phosphorous for microbial metabolism. In our study, no significant relationship was found between DNRA rates and *nrfA* gene abundance in eDNA, implying that extracellular compounds could not be responsible for DNRA activity despite the occurrence of *nrfA* gene in eDNA.

Ecological implications of DNRA in estuarine and intertidal wetlands

Dissimilatory nitrate reduction processes play an important role in controlling nitrate fate and budget under the anoxic and reduced conditions (Roberts et al. 2014; Bernard et al. 2015; Hardison et al. 2015; Robertson et al. 2016). In estuarine and intertidal wetlands, the importance and variability of nitrate reduction processes vary significantly in response to the oxic and anoxic fluctuations as a result of tidal flooding and ebb and vegetation intrusion. Thus, more studies are required to provide the information on the relative importance of nitrate reduction in estuarine and intertidal environments. In the present study, the potential rates of denitrification and anaerobic ammonium oxidation (anammox) were also measured (supplementary methods, SI) to quantify the contribution of DNRA to total nitrate reduction (sum of DNRA, denitrification and anammox). Based on these measured nitrate reduction rates (Fig. S5), DNRA contributed 8.1–37% of the total nitrate reduction (Fig. S6). Interestingly, although there was a great variability in DNRA rates between rhizosphere and non-rhizosphere soils of *Spartina alterniflora* ecotones, the mean contribution of DNRA to total nitrate reduction in both rhizosphere and non-rhizosphere soils accounted for roughly 20% of total reduction amount (Fig. S5), reflecting the considerable importance of DNRA to nitrate reduction in estuarine and intertidal wetlands. It was also noted that the contribution of DNRA to total nitrate reduction increased from the oligohaline to brackish sites, indicating that DNRA plays an increasing role in nitrate reduction in the estuarine environments. By integrating the available data of previous studies, we observed that the contribution of DNRA to total nitrate reduction logarithmically decreases with the increasing nitrate contents across the estuarine and coastal ecosystems ($r = 0.67$, $p < 0.05$, Fig. 7). The dissimilatory nitrate reduction processes, including denitrification, anammox and DNRA, can compete each other, depending on the differences of nitrate and organic matter availability (Koop-Jakobsen and Giblin 2010; Hardison et al. 2015; Kessler et al. 2018). DNRA can outcompete denitrification in the in the organic matter-enriched and nitrate-limited environments (Hardison et al. 2015). In addition, anammox can compete over DNRA in the organic matter-limited environments (Gu et al. 2018). High content of ammonium favors anammox but inhibits DNRA, because DNRA is favorable to occur in the ammonium-limited environments (Bonaglia et al. 2016; Kessler et al. 2018). Overall, nitrate, ammonium and organic matter are the crucial factors affecting the importance of DNRA across the estuarine and intertidal wetlands. Therefore, the logarithmical relationship between the contribution of DNRA to total nitrate reduction and the contents of nitrate was likely attributed to the limited organic carbon in these aquatic environments.

In this study, the average DNRA rate in rhizosphere soils of *Spartina alterniflora* ecotones was 1.51 times higher than that in non-rhizosphere soils. Assuming that the soil bulk density was approximately 2.68 g cm^{-3} (Yin et al. 2014), *Spartina alterniflora* soil had the potential capacity of 33.7 t N km^{-2} $yr.^{-1}$ converting nitrate into ammonium through DNRA, while nitrogen conversion capacity in bare flat was roughly 22.3 t N km^{-2} $yr.^{-1}$. Thus, the changes in intertidal habitats could cause a great increase in inorganic nitrogen retention because of *Spartina alterniflora* invasion. Over the past 30 years, China coastal zone has covered roughly 344.5 km^2 area of *Spartina alterniflora* invasion (Zuo et al. 2012). On the basis of DNRA capacities in rhizosphere and non-rhizosphere soils, the conversion of intertidal wetlands to *Spartina alterniflora* habitat would lead to a strong increase in nitrogen retention potential of 3916 t N $yr.^{-1}$ in China coastal zones. This estimation thus reflects an important ecological implication for bioavailable nitrogen source induced by *Spartina alterniflora* invasion in estuarine and intertidal wetlands. However, there may be an overestimation of DNRA rate and its environmental importance because

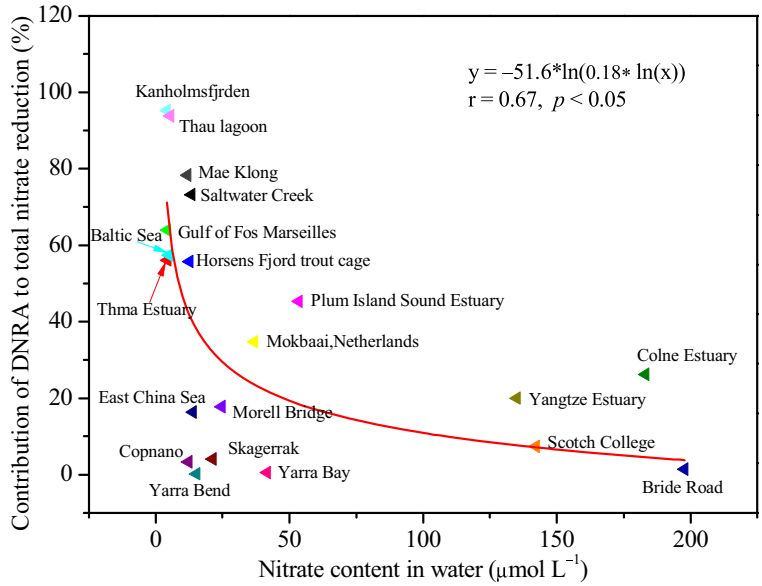

Fig. 7 Correlation of the contribution of DNRA to total nitrate reduction with nitrate contents in water of the Yangtze Estuary and other estuarine and coastal environments (Gilbert et al. 1997; Nishio et al. 1982; Goeyens et al. 1987; Bonin et al. 1998; Christensen et al. 2000; Thamdrup and Dalsgaard 2002; Karlson et al. 2005; Hietanen and Kuparinen 2008; Dong et al. 2009, 2011; Koop-Jakobsen and Giblin 2009; Jäntti and Hietanen 2012; Hou et al. 2012; Dunn et al. 2013; Song et al. 2013; Roberts et al. 2014; Robertson et al. 2016)

DNRA rates measured by the stimulated microbial bacteria may be higher in the slurry incubation than in situ field soils. The estimated broad-scale capacity of nitrogen retention was only based on the limited samples in our study. Actually, there are large spatial and temporal heterogeneities in soil substrates and DNRA rates across *Spartina alterniflora* ecotones. In addition, our estimation missed the vertical variation in DNRA rates within the soil depth affected by *Spartina alterniflora*. Thus, DNRA rates for extrapolating nitrogen retention could result in an uncertainty in China coastal wetlands.

In addition to the vegetation effects on biogeochemical cycling, it is noteworthy that salinity plays a strong influence on the carbon and nitrogen cycling under the sea level rise and seawater intrusion, resulting in a series of changes including sulfide production, dissolved oxygen potential and substrates availability (Morrissey et al. 2014; Robertson et al. 2016; Zhou et al. 2017). Salinity can accelerate carbon decomposition, extracellular enzyme activity and bacterial abundance (Morrissey et al. 2014), which may further affect the nitrogen cycling in estuarine and intertidal wetlands (Osborne et al. 2015). It has been reported that the increasing salinity can enhance denitrification and anammox and associated nitrogen loss in estuarine and intertidal environments (Hou et al. 2013). Thus, if the increasing salinity does stimulate biogeochemical cycling, it is difficult to examine how vegetation invasion regulates the nitrogen cycling in estuarine and intertidal wetlands (Hinshaw et al. 2017). However, as indicated in previous studies, the targeted work on salinity gradient approaches used to identify the influences of salinity on DNRA activity and associated microbial community is rare, and more importantly, this limited information can exactly evidence the responses of microbial metabolism, substrate supply and ionic availability to salinity dynamics in estuarine and intertidal wetlands. Therefore, more studies on the mechanisms underlying the salinity in relation to abiotic and biotic parameters are required to better predict the vegetation-induced changes in nitrogen cycling in estuarine and intertidal ecosystems.

Conclusions

In this study, we examined the effects of soil abiotic and biotic variables on DNRA activity and *nrfA* gene abundance in intertidal wetlands of the Yangtze Estuary. The dynamics of DNRA rates indicated that *Spartina alterniflora* invasion could facilitate DNRA activity through improving soil substrates availability and extracellular enzyme activity at the oligohaline sites, and salinity played a crucial role in shaping the DNRA process at the brackish sites. TOC, NO_3^-, Fe (II) and sulfide were the most important variables regulating DNRA activity in estuarine and intertidal wetlands. DNRA rates were more strongly stimulated by the abiotic and biotic parameters in *Spartina alterniflora* ecotones compared with *nrfA* gene abundance. DNRA has a great potential to convert nitrate into ammonium at a

rate of 3916 t N yr.$^{-1}$ after *Spartina alterniflora* invasion in China coastal zones. Overall, this study suggests that soil substrates have more influence on DNRA activity than gene abundance in *Spartina alterniflora* ecotones of estuarine and intertidal wetlands. Our results indicate that DNRA is of great significance in regulating nitrogen cycling, and highlight the importance of *Spartina alterniflora* in controlling the dynamics of DNRA in estuarine and intertidal wetlands.

Acknowledgments This work was supported by the National Natural Science Foundation of China (Nos. 41725002, 41701548, 41761144062 and 41671463), the Foundation for Excellent Youth Scholar of Fujian Normal University, the Fundamental Research Funds for the Central Universities, Chinese National Key Programs for Fundamental Research and Development (Nos. 2016YFA0600904 and 2016YFE0133700), and Royal Netherlands Academy of Arts and Sciences (No. PSA-SA-E-02). It was also funded by Key Laboratory of Yangtze River Water Environment, Ministry of Education (Tongji University), China (No. YRWEF201804). We thank the two anonymous reviewers for their constructive comments on the early version of this manuscript.

References

An S, Gardner WS (2002) Dissimilatory nitrate reduction to ammonium (DNRA) as a nitrogen link, versus denitrification as a sink in a shallow estuary (Laguna Madre/Baffin Bay, Texas). Mar Ecol Prog Ser 237(4):41–50

Bernard RJ, Mortazavi B, Kleinhuizen AA (2015) Dissimilatory nitrate reduction to ammonium (DNRA) seasonally dominates NO_3^- reduction pathways in an anthropogenically impacted sub-tropical coastal lagoon. Biogeochemistry 125(1): 47–64

Bonaglia S, Klawonn I, De Brabandere L, Deutsch B, Thamdrup B, Brüchert V (2016) Denitrification and DNRA at the Baltic Sea oxic–anoxic interface: substrate spectrum and kinetics. Limnol Oceanogr 61(5):1900–1915

Bonin P, Omnes P, Chalamet A (1998) Simultaneous occurrence of denitrification and nitrate ammonification in sediments of the French Mediterranean coast. Hydrobiologia 389(1–3): 169–182

Brookes PC, Landman A, Pruden G, Jenkinson DS (1985) Chloroform fumigation and the release of soil nitrogen: a rapid direct extraction method to measure microbial biomass nitrogen in soil. Soil Biol Biochem 17:837–842

Canfield DE, Glazer AN, Falkowski PG (2010) The evolution and future of Earth's nitrogen cycle. Science 330(6001):192–196

Canion A, Overholt WA, Kostka JE, Huettel M, Lavik G, Kuypers MM (2014) Temperature response of denitrification and anaerobic ammonium oxidation rates and microbial community structure in Arctic fjord sediments. Environ Microbiol 16: 3331–3344

Chen X, Zhong Y (1998) Coastal erosion along the Changjiang deltaic shoreline, China: history and prospective. Estuar Coast Shelf Sci 46:733–742

Christensen PB, Rysgaard S, Sloth NP, Christensen PB, Rysgaard S, Sloth NP, Dalsgaard T, Schwaerter S (2000) Sediment mineralization, nutrient fluxes, denitrification and dissimilatory nitrate reduction to ammonium in an estuarine fjord with sea cage trout farms. Aquat Microb Ecol 257(21):73–84

Church JA, White NJ (2006) A 20th century acceleration in global sea-level rise. Geophys Res Lett 33:L01602

Craft C (2007) Freshwater input structures soil properties, vertical accretion, and nutrient accumulation of Georgia and US tidal marshes. Limnol Oceanogr 52:1220–1230

Crowe SA, Canfield DE, Mucci A, Sundby B, Maranger R (2012) Anammox, denitrification and fixed-nitrogen removal in sediments from the lower St.. Lawrence Estuary. Biogeosciences 9:4309–4321

Decleyre H, Heylen K, Van Colen C, Willems A (2015) Dissimilatory nitrogen reduction in intertidal sediments of a temperate estuary: small scale heterogeneity and novel nitrate-to-ammonium reducers. Front Microbiol 6:1124

Deegan LA, Johnson DS, Warren RS, Peterson BJ, Fleeger JW, Fagherazzi S, Wollheim WM (2012) Coastal eutrophication as a driver of salt marsh loss. Nature 490(7420):388–392

Dell'Anno A, Stefano B, Danovaro R (2002) Quantification, base composition, and fate of extracellular DNA in marine sediments. Limnol Oceanogr 47(3):899–905

Deng FY, Hou LJ, Liu M, Zheng YL, Yin GY, Li XF, Lin XB, Chen F, Gao J, Jiang XF (2015) Dissimilatory nitrate reduction processes and associated contribution to nitrogen removal in sediments of the Yangtze estuary. J Geophys Res 120: 1521–1531

Domangue RJ, Mortazavi B (2018) Nitrate reduction pathways in the presence of excess nitrogen in a shallow eutrophic estuary. Environ Pollut 238:599–606

Dong LF, Smith CJ, Papaspyrou S, Stott A, Osborn AM, Nedwell DB (2009) Changes in benthic denitrification, nitrate ammonification, and anammox process rates and nitrate and nitrite reductase gene abundances along an estuarine nutrient gradient (the Colne estuary, United Kingdom). Appl Environ Microbiol 75(10):3171–3179

Dong LF, Sobey MN, Smith C, Rusmana I, Phillips W, Stott A, Osborn AM, Nedwell DB (2011) Dissimilatory reduction of nitrate to ammonium (DNRA) not denitrification or anammox dominates benthic nitrate reduction in tropical estuaries. Limnol Oceanogr 56:279–291

Dotaniya ML, Meena VD (2015) Rhizosphere effect on nutrient availability in soil and its uptake by plants: a review. P Natl A Sci India B 85(1):1–12

Du YH, Guo P, Liu JQ, Wang CY, Yang N, Jiao ZX (2014) Different types of nitrogen deposition show variable effects on the soil carbon cycle process of temperate forests. Glob Chang Biol 20(10):3222–3228

Dunn RJ, Robertson D, Teasdale PR, Waltham NJ, Welsh DT (2013) Benthic metabolism and nitrogen dynamics in an urbanized tidal creek: domination of DNRA over denitrification as a nitrate reduction pathway. Estuar Coast Shelf Sci 131:271–281

Fernandes SO, Michotey VD, Guasco S, Bonin PC, Bharathi PAL (2012) Denitrification prevails over anammox in tropical mangrove sediments (Goa, India). Mar Environ Res 74:9–19

Gao DZ, Li XF, Lin XB, Wu DM, Jin BS, Huang YP, Liu M, Chen X (2017) Soil dissimilatory nitrate reduction processes in the Spartina alterniflora invasion chronosequences of a coastal wetland of southeastern China: Dynamics and environmental implications. Plant Soil 421(1-2):383–399

Gardner WS, McCarthy MJ (2009) Nitrogen dynamics at the sediment-water interface in shallow, sub-tropical Florida bay: why denitrification efficiency may decrease with increased eutrophication. Biogeochemistry 95(2/3):185–198

Gardner WS, McCarthy MJ, An S, Sobolev D, Sell KS, Brock D (2006) Nitrogen fixation and dissimilatory nitrate reduction to ammonium (DNRA) support nitrogen dynamics in Texas estuaries. Limnol Oceanogr 51:558–568

Giblin AE, Weston NB, Banta GT, Tucker J, Hopkinson CS (2010) The effects of salinity on nitrogen losses from an oligohaline estuarine sediment. Estuar Coasts 33:1054–1068

Giblin AE, Tobias CR, Song BK, Weston N, Banta GT, Rivera-Monroy VH (2013) The importance of dissimilatory nitrate reduction to ammonium (DNRA) in the nitrogen cycle of coastal ecosystems. Oceanography 26(3):124–131

Gilbert F, Souchu P, Bianchi M, Bonin P (1997) Influence of shellfish farming activities on nitrification, nitrate reduction to ammonium and denitrification at the water-sediment interface of the Thau lagoon, France. Mar Ecol Prog Ser 151:143–153

Goeyens L, De Vries RTP, Bakker JF, Helder W (1987) An experiment on the relative importance of denitrification, nitrate reduction and ammonification in coastal marine sediment. J Sea Res 21(3):171–175

Greaver TL, Clark CM, Comptonm JE, Vallano D, Talhelm AF, Weaver CP, Band LE, Baron JS, Daavidson EA, Tague CL, Felker-quinn E, Lynch JA, Herrick JD, Liu L, Goddale CL, Novak KJ, Haeuber RA (2016) Key ecological responses to nitrogen are altered by climate change. Nat Clim Chang 6(9): 836–843

Gu ZL, Li Y, Yang YF, Xia SQ, Hermanowicz SW, Alvarez-Cohen L (2018) Inhibition of anammox by sludge thermal hydrolysis and metagenomic insights. Bioresour Technol 270:46–54

Hardison AK, Algar CK, Giblin AE, Rich JJ (2015) Influence of organic carbon and nitrate loading on partitioning between dissimilatory nitrate reduction to ammonium (DNRA) and N_2 production. Geochim Cosmochim Acta 164:146–160

He Y, Widney S, Ruan M, Herbert E, Li X, Craft C (2016) Accumulation of soil carbon drives denitrification potential and lab incubated gas production along a chronosequence of salt marsh development. Estuar Coast Shelf Sci 172:72–80

Henry S, Texier S, Hallet S, Bru D, Dambreville C, Chèneby D, Bizouard F, Germon JC, Philippot L (2008) Disentangling the rhizosphere effect on nitrate reducers and denitrifiers: insight into the role of root exudates. Environ Microbiol 10(11):3082–3092

Hietanen S, Kuparinen J (2008) Seasonal and short-term variation in denitrification and anammox at a coastal station on the Gulf of Finland, Baltic Sea. Hydrobiologia 596(1):67–77

Hinshaw SE, Tatariw C, Flournoy N, Kleinhuizen A, Taylor C, Sobecky PA, Mortazavi B (2017) Vegetation loss decreases salt marsh denitrification capacity: implications for marsh erosion. Environ Sci Technol 51(15):8245–8253

Hou LJ, Liu M, Carini SA, Gardner WS (2012) Transformation and fate of nitrate near the sediment–water interface of Copano Bay. Cont Shelf Res 35:86–94

Hou LJ, Zheng YL, Liu M, Gong J, Zhang XL, Yin GY, You L (2013) Anaerobic ammonium oxidation (anammox) bacterial diversity, abundance, and activity in marsh sediments of the Yangtze estuary. J Geophys Res 118:1237–1246

Jäntti H, Hietanen S (2012) The effects of hypoxia on sediment nitrogen cycling in the Baltic Sea. Ambio 41(2):161–169

Jian SY, Li JW, Chen J, Wang GS, Mayes MA, Dzantor KE, Dzantor KE, Hui DF, Luo YQ (2016) Soil extracellular enzyme activities, soil carbon and nitrogen storage under nitrogen fertilization: a meta-analysis. Soil Biol Biochem 101:32–43

Karlson K, Hulth S, Ringdahl K, Rosenberg R (2005) Experimental recolonisation of Baltic Sea reduced sediments: survival of benthic macrofauna and effects on nutrient cycling. Mar Ecol Prog Ser 294:35–49

Kessler AJ, Roberts KL, Bissett A, Cook PL (2018) Biogeochemical controls on the relative importance of denitrification and dissimilatory nitrate reduction to ammonium in estuaries. Glob Biogeochem Cycles 32:1045–1057

Kirwan ML, Megonigal JP (2013) Tidal wetland stability in the face of human impacts and sea-level rise. Nature 504:53–60

Koop-Jakobsen K, Giblin AE (2009) Anammox in tidal marsh sediments: the role of salinity, nitrogen loading, and marsh vegetation. Estuar Coasts 32(2):238–245

Koop-Jakobsen K, Giblin AE (2010) The effect of increased nitrate loading on nitrate reduction via denitrification and DNRA in salt marsh sediments. Limnol Oceanogr 55:789–802

Liu JE, Han RM, Su HR, Wu YP, Zhang LM, Richardson CJ, Wang GX (2017a) Effects of exotic *Spartina alterniflora* on vertical soil organic carbon distribution and storage amount in coastal salt marshes in Jiangsu, China. Ecol Eng 106:132–139

Liu X, Ruecker A, Song B, Xing J, Conner WH, Chow AT (2017b) Effects of salinity and wet–dry treatments on C and N dynamics in coastal-forested wetland soils: implications of sea level rise. Soil Biol Biochem 112:56–67

Lovley DR, Phillips EJP (1987) Rapid assay for microbially reducible ferric iron in aquatic sediments. Appl Environ Microbiol 53:1536–1540

Mao D, Luo Y, Mathieu J, Wang Q, Feng L, Mu Q, Feng CY, Alvarez PJJ (2013) Persistence of extracellular DNA in river sediment facilitates antibiotic resistance gene propagation. Environ Sci Technol 48(1):71–78

Mohan SB, Schmid M, Jetten M, Cole J (2004) Detection and widespread distribution of the *nrfA* gene encoding nitrite reduction to ammonia, a short circuit in the biological nitrogen cycle that competes with denitrification. FEMS Microbiol Ecol 49:433–443

Morrissey EM, Gillespie JL, Morina JC, Franklin RB (2014) Salinity affects microbial activity and soil organic matter content in tidal wetlands. Glob Chang Biol 20:1351–1362

Nielsen KM, Johnsen PJ, Bensasson D, Daffonchio D (2007) Release and persistence of extracellular DNA in the environment. Environ Biosaf Res 6(1–2):37–53

Nishio T, Koike I, Hattori A (1982) Denitrification, nitrate reduction, and oxygen consumption in coastal and estuarine sediments. Appl Environ Microbiol 43(3):648–653

Noe GB, Krauss KW, Lockaby BG, Conner WH, Hupp CR (2013) The effect of increasing salinity and forest mortality on soil nitrogen and phosphorus mineralization in tidal freshwater forested wetlands. Biogeochemistry 114:225–244

Osborne RI, Bernot MJ, Findlay SE (2015) Changes in nitrogen cycling processes along a salinity gradient in tidal wetlands of the Hudson River, New York, USA. Wetlands 35(2):323–334

Pietramellara G, Ascher J, Borgogni F, Ceccherini MT, Guerri G, Nannipieri P (2009) Extracellular DNA in soil and sediment: fate and ecological relevance. Biol Fertil Soils 45(3):219–235

Rasmussen P, Sonnenborg TO, Goncear G, Hinsby K (2013) Assessing impacts of climate change, sea level rise, and drainage canals on saltwater intrusion to coastal aquifer. Hydrol Earth Syst Sci 17:421–443

Roberts KL, Kessler AJ, Grace MR, Cook PL (2014) Increased rates of dissimilatory nitrate reduction to ammonium (DNRA) under oxic conditions in a periodically hypoxic estuary. Geochim Cosmochim Acta 133:313–324

Robertson EK, Roberts KL, Burdorf LD, Cook P, Thamdrup B (2016) Dissimilatory nitrate reduction to ammonium coupled to Fe (II) oxidation in sediments of a periodically hypoxic estuary. Limnol Oceanogr 61(1):365–381

Saeki K, Kunito T, Sakai M (2010) Effects of pH, ionic strength, and solutes on DNA adsorption by andosols. Biol Fertil Soils 46(5):531–535

Smith CJ, Nedwell DB, Dong LF, Osborn AM (2007) Diversity and abundance of nitrate reductase genes *(nar G* and *napA*), nitrite reductase genes (*nirS* and *nrfA*), and their transcripts in estuarine sediments. Appl Environ Microbiol 73:3612–3622

Smith CJ, Dong LF, Wilson J, Stott A, Osborn AM, Nedwell D (2015) Seasonal variation in denitrification and dissimilatory nitrate reduction to ammonia process rates and corresponding key functional genes along an estuarine nitrate gradient. Front Microbiol 6:542

Song GD, Liu SM, Marchant H, Kuypers MMM, Lavik G (2013) Anammox, denitrification and dissimilatory nitrate reduction to ammonium in the East China Sea sediment. Biogeosciences 10(11):6851–6864

Song BK, Lisa JA, Tobias CR (2014) Linking DNRA community structure and activity in a shallow lagoonal estuarine system. Front Microbiol 5:460

Tabatabai M (1994) Soil enzymes. In: Weaver R, Angle J, Bottomley P (eds) Methods of soil analysis, part 2: microbiological and biochemical properties. Soil Science Society of America, Madison, pp 775–833

Tang YS, Wang L, Jia JW, Li YL, Zhang WQ, Wang HL, Sun Y (2011) Response of soil microbial respiration of tidal wetlands in the Yangtze River estuary to different artificial disturbances. Ecol Eng 37:1638–1646

Thamdrup B, Dalsgaard T (2002) Production of N_2 through anaerobic ammonium oxidation coupled to nitrate reduction in marine sediments. Appl Environ Microbiol 68(3):1312–1318

Van de Broek M, Vandendriessche C, Poppelmonde D, Merckx R, Temmerman S, Govers G (2018) Long-term organic carbon sequestration in tidal marsh sediments is dominated by old-aged allochthonous inputs in a macrotidal estuary. Glob Chang Biol 24:2498–2512. https://doi.org/10.1111/gcb.14089

Vance ED, Brookes PC, Jenkinson DS (1987) An extraction method for measuring soil microbial biomass C. Soil Biol Biochem 19:703–707

Xiao W, Chen X, Jing X, Zhu B (2018) A meta-analysis of soil extracellular enzyme activities in response to global change. Soil Biol Biochem 123:21–32

Yin GY, Hou LJ, Liu M, Liu ZF, Gardner WS (2014) A novel membrane inlet mass spectrometer method to measure $^{15}NH_4^+$ for isotope-enrichment experiments in aquatic ecosystems. Environ Sci Technol 48(16):9555–9562

Zhang YH, Ding WS, Luo JF, Donnison A (2010) Changes in soil organic carbon dynamics in an eastern Chinese coastal wetland following invasion by a C_4 plant *Spartina alterniflora*. Soil Biol Biochem 42:1712–1720

Zhou M, Butterbach-Bahl K, Vereecken H, Brüggemann N (2017) A meta–analysis of soil salinization effects on nitrogen pools, cycles and fluxes in coastal ecosystems. Glob Chang Biol 23(3):1338–1352

Zuo P, Zhao SH, Liu CA, Wang CH, Liang YB (2012) Distribution of *Spartina spp*. along China's coast. Ecol Eng 40:160–166